

Instanton Supported Scalar Hair on Black Holes

Jennie Traschen and K. Z. Win^y

Department of Physics and Astronomy
University of Massachusetts
Amherst, MA 01003

We present analytical perturbative, and numerical solutions of the Einstein equation which describe a black hole with a nontrivial dilaton field and a purely topological gauge potential. The gauge potential has zero field strength and hence no stress-energy, but it does couple to virtual string worldsheets which wrap around the Euclidean horizon two-sphere, and generate an effective interaction in the spacetime lagrangian. We use the lagrangian with a nonstandard potential for a scalar field that reproduces the effect of the worldsheet instantons. As has been previously pointed out the topological charge Q of the gauge field can be detected by an Aharonov-Bohm type experiment using quantum strings; the classical scalar hair of the solutions here is a classical detection of Q . ADM mass, dilaton charge and Hawking temperature are calculated and compared with the known cases when appropriate. We discuss why these solutions do not violate the no-hair theorems and show that, for sufficiently small interaction coupling, the solutions are stable under linear time dependent perturbations.

February 1997

lboo@phast.umass.edu

^y win@phast.umass.edu

1. Introduction

The no-hair theorems in the physics of black holes essentially state that the only physical parameters describing a black hole are its mass, angular momentum, and conserved charges associated with long range fields. Originally no-hair theorems arose from the uniqueness theorems of Israel, Carter and Wald [1] for the Kerr solution. If the cosmic censorship conjecture is correct, and hence the gravitational collapse of a star gives rise to a black hole, the no-hair theorems imply that the black hole must be described by the Kerr solution. An alternative method of proving a no-hair theorem, developed by Bekenstein [2] is to show that the black hole geometry cannot support nontrivial classical field configurations that are of interest. We review this in section 5. In particular, a no-hair theorem must be proved (or disproved) for each matter theory of interest. For a scalar field coupled to gravity, there are simple proofs when either the potential energy $V(\phi)$ or $\partial V/\partial\phi$ is positive definite polynomial. So scalar hair is ruled out for the standard self interacting potential $V(\phi) = \frac{1}{2}m^2\phi^2 + \frac{\lambda}{4}\phi^4$ if $m^2 > 0$. The important case of spontaneous symmetry breaking, when $m^2 < 0$ and ϕ is coupled to a gauge field, requires a more careful argument, and is first proved in [3].

In recent years, however, black holes with various kinds of hair have been discovered. The "colored" black hole supporting Yang-Mills gauge field was first numerically discovered [4], and existence was later proven analytically [5]. The colored black hole possesses zero Yang-Mills charge and thus parametrized only by its ADM mass. Further, it was shown [6] that a black hole can exist inside a magnetic monopole of spontaneously broken gauge theories. Under much more generality it was shown in [7] that black holes can exist inside various classical field configurations of which magnetic monopole is only a special case. The charged dilaton black holes [8][9] carry electric and magnetic charges, and also have nontrivial scalar fields. Now, in all these examples of black holes with scalar hair, the black hole also carries electric and/or magnetic charges. In this paper, we present numerical solutions, and analytic perturbative solutions, for black holes with nontrivial dilaton field, but no electric or magnetic charge. Instead, the black hole has a topological "axion" charge, that is, there is a nontrivial 2-form gauge potential B_{ab} , with vanishing field strength, that wraps around the horizon two-sphere. Classically B_{ab} is not observable; its existence can be inferred by a distant observer, by the nontrivial scalar field on the black hole.

These are asymptotically flat versions of the black holes constructed by Giddings et.al. [10] and are the solutions to bosonic string theory, which correspond to black holes with a dilaton and a purely topological axion gauge potential. However, these exact solutions are "all throat," i.e. the radius of two sphere is constant. The authors write down a spacetime lagrangian which contains an effective potential giving the effect of Euclidean string world sheets that couple to the gauge potential and wrap around the horizon two-sphere. It is this interaction term which allows one to get around the usual no hair construction. Hence the classically observable scalar hair is supported by the classically unobservable world sheet instantons.

In classical electrodynamics the gauge invariant field strength is the physically observable quantity. However in quantum mechanics the potential can affect a particle even in those regions where the field strength is identically zero, as illustrated in the famous Aharonov-Bohm effect. A similar phenomenon comes up in string theory. A string naturally couples to a 2-form potential, B_{ab} , since its trajectory is described by a world sheet. $H_{abc} (= \partial_a B_{bc} + \text{cyclic terms})$ is the gauge invariant quantity and determines the classical equation of motion. The static spherically symmetric solution of an axion field interacting with gravity is the Schwarzschild metric supplemented by an axion potential with a nonzero component given by [11] $B = \frac{Q}{2} \sin^2\theta$ where Q is a constant. It follows that $H = 0$ and no classical measurement outside the black hole could determine the axion charge of a black hole. However as pointed out in [11] if two strings originating at the same spacetime point are made to interfere at another spacetime point with the volume enclosed

by two world sheets enclosing the black hole, the quantum phase difference, between two strings at the end of their trajectory will be proportional to Q . Thus Q becomes a new observable quantity of the system despite the fact that strings world sheet do not touch the region of nonzero H . This observable could be considered a new kind of quantum hair for black holes.

The Anharmonic-Bohm type experiment described above for strings would be difficult to perform. If the axion field were coupled to another auxiliary field, such as the dilaton, one might infer axion charge by measuring the auxiliary field. Interestingly one can give such an interpretation to an effective spacetime action describing the interaction between gravity, the axion and the dilaton derived by Giddings et al. [10]. In their work an exact classical solution of bosonic string theory is found as a conformally invariant sigma model, containing both the symmetric metric coupling, and an antisymmetric coupling $B = Q \sin \theta = 2$. A fixed point of that theory occurs when $Q = 1$. These exact solutions found in [10] can be interpreted as a black hole geometry without an asymptotically flat region. As such their solution cannot describe a black hole found in our spacetime. However, on large scales the system can be studied using a spacetime action with the world-sheet instanton effects included by an effective interaction [10]. In the rest of the paper we investigate the existence of asymptotically flat solutions using this spacetime action.

2. Equations of Motion and Boundary Conditions

We will write the static spherically symmetric Einstein metric as

$$ds^2 = -f(r)dt^2 + \frac{dr^2}{A(r)} + R^2(r)d\Omega^2 \quad (2.1)$$

The four-dimensional low-energy effective action obtained in [10] for $Q = 1$ is

$$S = \int d^4x \left[\frac{1}{2g^2} (R + 2(\sigma')^2 + V(\sigma)) \right]$$

where σ is the dilaton field and V reproduces the effect of the world sheet instantons which couple to the topological gauge potential B ,

$$V(\sigma) = \frac{2C}{r^2} e^{2\sigma - 2R^2(r) = 0} \quad (2.2)$$

Note that we are using the Einstein metric, whereas in [10] the string metric is used, dimensionally reduced to the t - r plane.

In (2.2), C is a positive constant which comes from the determinant of fluctuations about the instantons. Hence C naturally arises as a small parameter, and this suggests using a perturbative approach to look for solutions which are almost Schwarzschild black holes, with a small but nonconstant dilaton. We first find these solutions, and then turn to the exact case.

After choosing the gauge $R = r$, we obtain three independent equations of motion, with $r = x r_h$

$$A x^2 \omega = (1 + x^{-2}) C e^{2\sigma - 2r_h^2} (1 + A) x^{-2} \quad (2.3)$$

$$A^0 x = 1 - A - A x^2 \omega - C e^{2\sigma - 2r_h^2} \quad (2.4)$$

$$(\ln f)^0 = 2x^{-2} + (\ln A)^0 \quad (2.5)$$

where primes denote differentiation with respect to x , and $2=^0$ has been scaled away. For asymptotically flat spacetime, we require

$$A; f \rightarrow 1 \quad 2M = r \quad \text{as } r \rightarrow 1 : \quad (2.6)$$

Requiring an event horizon at $r = r_h$ ($x = 1$) implies that

$$A_h = f_h = 0 \quad (2.7)$$

The subscript h will stand for quantities at $x = 1$. For a solution we require that ϕ is differentiable at r_h . The energy density, ρ , is given by $4\rho = 4T^t_t = (A^2 + C e^{2\phi} r^2) = 2$. Finiteness of ρ at r_h puts no further condition on ϕ . The total energy in the dilaton field outside the horizon is finite, $4\pi \int_{r_h}^{\infty} r^2 f A dr < \infty$, if ϕ vanishes asymptotically at least as fast as $1/r$ with $\gamma > 1.5$. By solving (2.3) asymptotically, we find that $\phi = 2$. Thus

$$\phi = 2 + O(1/r) \quad \text{as } r \rightarrow 1 \quad (2.8)$$

together with equation (2.6) constitute sufficient conditions for asymptotic flatness and finite total energy. To get a unique solution we must impose on a particular value of ϕ at infinity. We can require that

$$\phi_1 = 0 \quad (2.9)$$

though we will see in section 4 that if C is fixed there is a range of r_h and hence a range of ϕ_1 that leads to the asymptotically flat solutions. Alternatively we can impose (2.9), without loss of generality, for all solutions and let C vary in which case there will be a range of values of C that give (2.9). That there is one-to-one correspondence between the two parameters, ϕ_1 and C , can be easily seen from the fact that setting $C = 1$ amounts to redefining ϕ according to the scheme $C e^{2\phi} \rightarrow e^{2\phi}$. Each of the two parameters that one allows to vary has its own advantage. If one keeps ϕ_1 fixed and lets C vary, one can imagine turning on the perturbation potential V of the Schwarzschild black hole. But to discuss the existence of solution numerically it is more convenient to fix C and let ϕ_1 (or equivalently r_h) vary.

3. Perturbative Solutions

We observe first that when $C = 0$ the equations of motion for the metric functions are solved by the Schwarzschild spacetime. The equation for ϕ is that of a massless scalar field minimally coupled to gravity and is solved by the unique solution $\phi = \text{constant}$. For small C we look for a perturbative solution to the equations of motion. Non-existence of a perturbative solution would indicate that no exact solution exists while existence means only that the exact solution may exist.

Let the metric be that of Schwarzschild with $f = A = 1 - 2M/r$ and C and ϕ to be small quantities of the same order. The equation of motion for ϕ , $2r^2 \phi'' = V$, after scaling $r = x r_h$, becomes

$$[(x^2 - x) \phi']' = C e^{2\phi} x^2 r_h^2$$

which can be immediately integrated to obtain ϕ to first order in the small quantity

$$\phi = C \int_1^x \frac{G(t)}{t^2} dt$$

where $G(z) = \int_1^z e^{r_h^2 t^2} dt$. This solution satisfies all boundary conditions: $\frac{d\phi}{dx} \rightarrow 0$ as $x \rightarrow 1$, and ϕ is bounded and differentiable at r_h . It is also consistent with our assumption that ϕ and C are of the same order in the small quantity.

One can also compute the first order correction to the metric. If one lets $A = 1 - (1 + C) \phi = x$ then one can solve for ϕ using (2.4). One finds

$$\phi = G(x)$$

Since $\lim_{x \rightarrow 1} G(x) = \text{positive constant}$, this solution indicates that the presence of the dilaton field increases the ADM mass from the Schwarzschild value, a fact supported by the numerical solution found in the next section. From equation (2.5) it follows that $f = A$ to first order in C .

4. Numerical Results

For all cases considered in this section, we take $r_h = C = 1$ unless otherwise specified. For all other values of r_h we have tested, we find that numerical solutions also exist, but we do not have a proof that this is true in general. At the end of this section we discuss the parameter space of α and varying C .

Because equations (2.3) and (2.4) do not involve f we solve these two equations for A and ϕ and then use (2.5) to solve for f . Equations (2.3) and (2.4) are solved numerically with the boundary conditions (2.6), and (2.7) using the shooting method [12]. To start shooting, initial values must be chosen for A , ϕ , and f at r_h . But at $x = 1$, equation (2.3) gives a constraint between A_h and ϕ_h :

$$\phi_h^0 = 1 - (e^{r_h^2} - 2\alpha_h - 1) \quad (4.1)$$

Note that the solution in section 2 satisfies this constraint. For a given value of r_h we thus have only one shooting parameter, α_h . Equation (4.1) is singular when $2\alpha_h = r_h^2$. Indeed, a solution exists only when $2\alpha_h < r_h^2$, because the equation (2.4) gives

$$A_h^0 = 1 - e^{2\alpha_h - r_h^2} \quad (4.2)$$

and since $A_h = 0$ it is necessary that $A_h^0 > 0$ which is possible only if $2\alpha_h > r_h^2$.

One sees that A monotonically increases with x as follows. For $2\alpha_h > r_h^2$, $\phi_h^0 > 0$. Thus if there exists a local extremum of A for some $x = x_e > 1$ it must be a local maximum. However according to equation (2.3)

$$A(x_e)x_e^2 \phi(x_e) = e^{2\alpha(x_e) - x_e^2 r_h^2} > 0$$

ie. that local extremum can only be a local minimum. Therefore there can be no local extremum of A for any finite value of x .

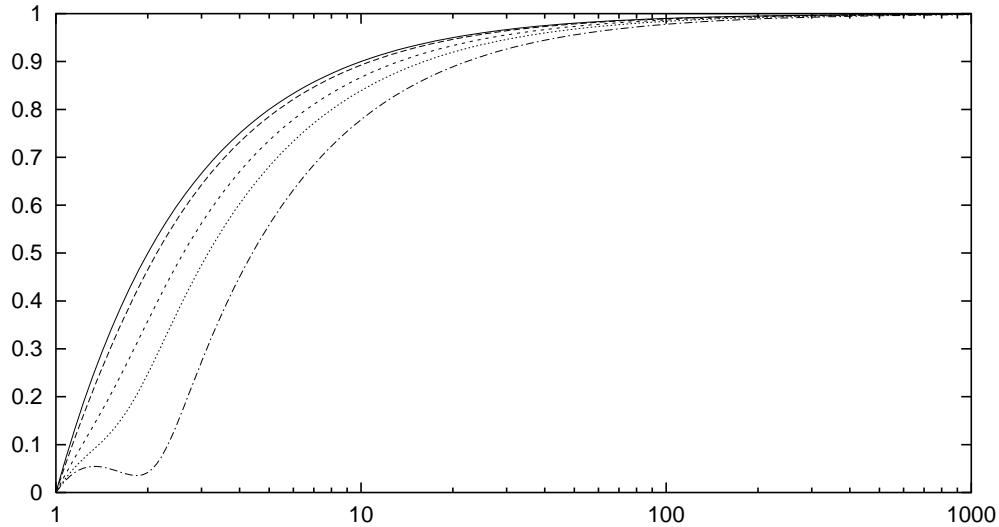


Figure 1. A vs. x $(r_h, C) = (1, 1)$

Solid line is the Schwarzschild solution, $1 = x$. For the dashed lines, from left to right, $\alpha_h = 0.4; 0.1; 0.2; 0.235$.

We find that for each r_h there is a range of $\alpha_h \in (1; \alpha_h^{\max}]$ that will give $\alpha_1 = \text{constant}$. For example for $r_h = 1$, $\alpha_h = 0.21678$ gives $\alpha_1 = 0$ and $\alpha_h^{\max} = 0.235596$. The relation between α_h^{\max} and r_h is summarized in figure 7. For all $\alpha_h < \alpha_h^{\max}$ monotonically increases to a constant value and A approaches the Schwartzschild result, $1 - 1/x$, asymptotically. Figure 1 also shows that A approaches Schwartzschild solution everywhere as $\alpha_h \rightarrow 1$. This is expected because $\alpha_h \rightarrow 1$ is the same as $C \rightarrow 0^+$.

Once A and α are known f can be integrated using equation (2.5). Note that (2.5) is linear in f . This is compatible with the fact that the time coordinate can be scaled by a constant. Because of the event horizon, (2.5) does not determine f_h^0 . Initially we take $f_h^0 = A_h^0$ which gives a solution such that $\lim_{r \rightarrow 1} f = f_1$. Further scaling of time coordinate is necessary to obtain $\lim_{r \rightarrow 1} f = 1$ i.e. for the final solution we pick $f_h^0 = A_h^0 = f_1$. f_h^0 is necessary for computing Hawking temperature later.

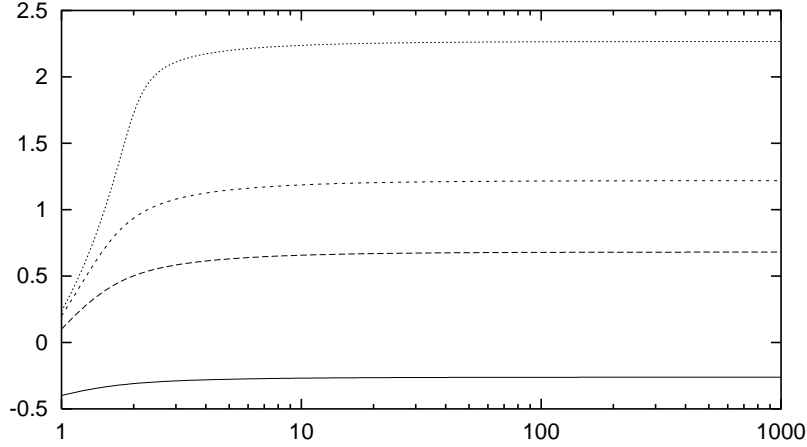


Figure 2. f vs. x $r_h = 1$

For the numerical analysis it is convenient to think of the solutions as being parametrized by $(r_h; \alpha_h)$. However, we may also consider the solutions as being parametrized by two global charges: the ADM mass, M , and the dilaton charge, D . We now turn to calculating these two charges.

The ADM mass can be read off of the large r behavior of A , $1 - 2M/r$. Figure 3 shows that for a fixed α_1 , ($M = M_{C=0}$) increases with C as noted with the perturbative solution.

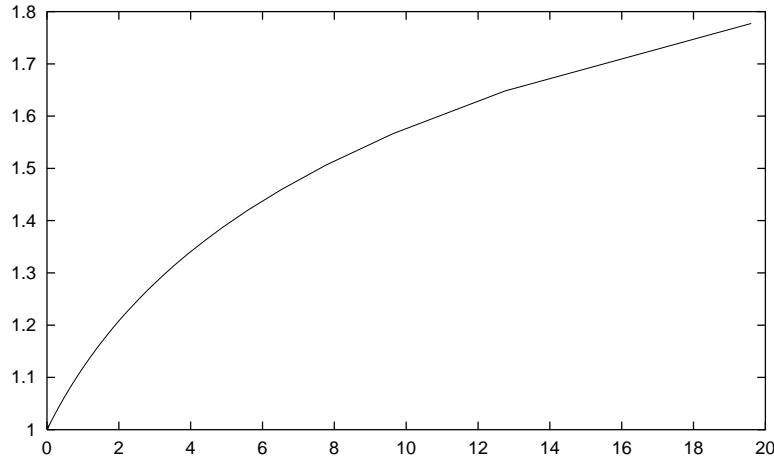


Figure 3. ($M = M_{C=0}$) vs. C $(r_h; \alpha_1) = (1; 0)$

A plot of $(x^2)^0$ vs. x in figure 4 shows that $(x^2)^0$ constant $= x^2$ as $x \rightarrow 1$. This asymptotic behavior agrees with that of perturbative solution and satisfies equation (2.8). With this behavior of $(x^2)^0$,

$$D = \frac{1}{4} \frac{d^2}{dr^2} r^2 = \frac{1}{4} \frac{d}{dr} r^2 \frac{d}{dr}$$

is finite. D should not be thought of as another free parameter. Figure 5 shows one-to-one correspondence between D and α_1 . Also there is one-to-one correspondence between two parameter spaces $(r_h; \alpha_1)$ and $(M; D)$.

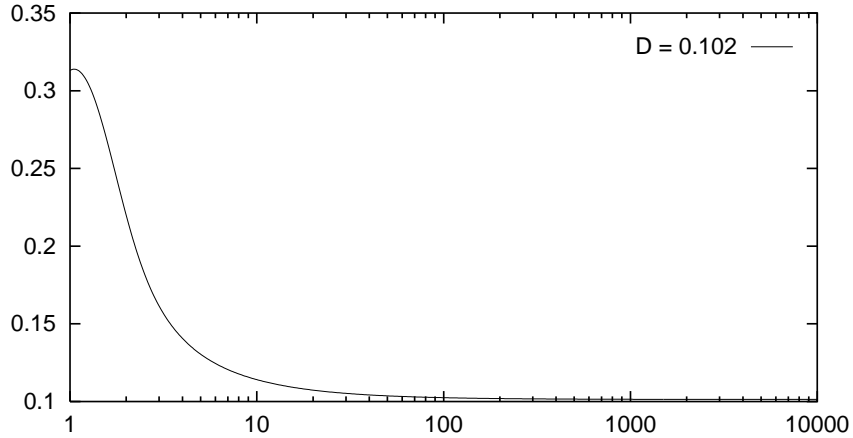


Figure 4. $(x^2)^0$ vs. x $(r_h; C; \alpha_1) = (1; 1; 0)$

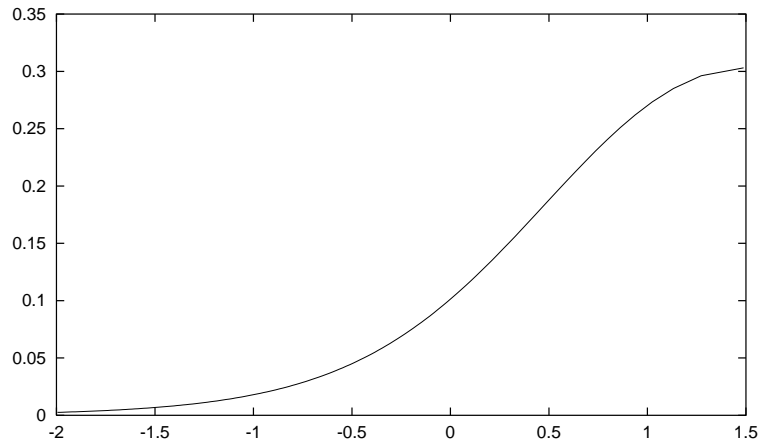


Figure 5. D vs. α_1 $(r_h; C) = (1; 1)$

Another quantity of interest is Hawking temperature, $T_H = \frac{\kappa}{2\pi}$ is surface gravity [1] and is given by $\lim_{r \rightarrow r_h} (V a)$ where $a = \frac{1}{\sqrt{-g_{tt}}}$, $a^c = (\frac{1}{\sqrt{-g_{tt}}})^c = (\frac{1}{\sqrt{-g_{tt}}})^c$, and $V = \frac{1}{\sqrt{-g_{rr}}}$. We find that

$$4 T_H = \lim_{r \rightarrow r_H} f^0 = \frac{1}{f_H} = \frac{1}{f_H^0 A_h^0} = A_h^0 = \frac{1}{f_1}$$

continuously decreases with α_1 , and hence with r_h . An alternative expression, obtained by using equation (4.2), $4 T_H = (1 - e^{2\alpha_1 r_h^2}) = \frac{1}{f_1}$ explains the decreasing of T_H with

r_h . It also supports our finding that no solution exists for large value of r_h because if $r_h > r_c$ $r_h^2 = 2$, T_H will be negative. Figure 7 shows the relation between r_h^{max} and r_h and it shows that as $r_h \rightarrow 1$, $r_h^{max} \rightarrow r_h^2 = 2 =$ Hawking temperature bound.

For a fixed r_h the effect of dilaton charge is to lower the Hawking temperature as evident by figure 6. In this respect the dilaton charge has a similar effect on the black hole as the electric or magnetic charge. Recall that the Hawking temperature of a Reissner-Nordstrom black hole is given by

$$4 T_H = \frac{r_+^2 - Q_{em}^2}{r_+^3}$$

where r_+ is the outer horizon radius, and Q_{em} the electric or magnetic charge of the black hole.

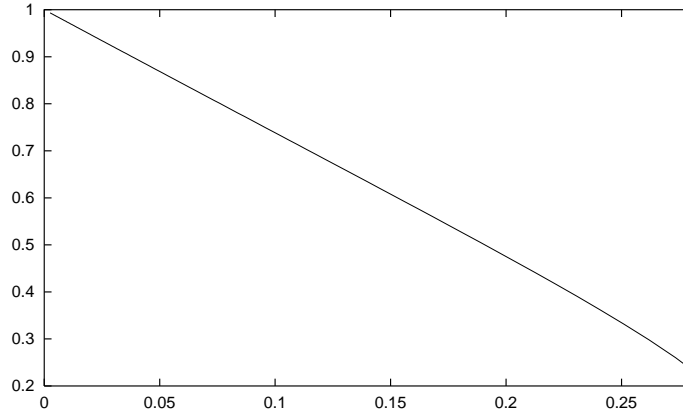


Figure 6. $4 T_H$ vs. D $r_h = 1$

Throughout this section we have taken $C = 1$ and found that the solution exists when $r_h \in (1; r_h^{max}]$ (or equivalently $r_1 \in (1; r_1^{max}]$.) As noted at the end of section 2 if e is the solution with $C = 1$ then e^C will be the solution for a different positive C where $e = \ln C$. If we demand that $e_1 = 0$ always, then for a fixed r_h the solution exists if and only if $C \in [0; C^{max}]$ where $C^{max} = e^{2/r_h^{max}}$. It can be easily verified that picking $e_h = r_h - 1$ and $C = e^{2/r_h}$ will ensure $e_1 = 0$.

5. Consistency with No-Hair Theorems

To check whether black hole solutions we found are consistent with various no-hair theorems we review the proofs such theorems. Consider a theory of scalar field interacting with gravity described by the action, $S = \int [R + (r')^2 + V(\phi; x)] \sqrt{-g} d^4x$. If we write the line element in the form of (2.1) with $R = r$ the equation of motion is $\frac{1}{r^2} \frac{d}{dr} (r^2 \frac{d\phi}{dr}) = -\frac{\partial V}{\partial \phi}$ where primes denote d/dr . Now for asymptotic flatness we can consistently require $\lim_{r \rightarrow \infty} \phi = 0$. Multiplying both sides by ϕ and integrating by parts gives $\frac{1}{r^2} \frac{d}{dr} (r^2 \phi \frac{d\phi}{dr}) = -\phi \frac{\partial V}{\partial \phi} + \frac{\partial V}{\partial \phi} \phi = -\phi \frac{\partial V}{\partial \phi}$. The left side is zero on account of the boundary conditions imposed at r_h and ∞ . If $\frac{\partial V}{\partial \phi}$ is positive definite for $r > r_h$, then the integrand is positive definite and we see that for such forms of $V(\phi)$ the only solution for ϕ is the trivial one: $\phi = 0$. However, for the interaction V we use $\frac{\partial V}{\partial \phi}$ is not necessarily positive definite.

No-hair theorems using scaling arguments [13] impose slightly different condition, namely, that V itself be positive definite. It appears at first sight that V we use satisfies this condition. However the proof in [13] makes use of the fact that V does not depend on coordinates explicitly which our V clearly does not satisfy.

6. Stability Analysis

To study the stability of the solution, we will consider spherically symmetric perturbations around the static solution. We will show that the solution is stable for sufficiently small C . Let

$$f(r;t) = f_0(r) + \delta f(r;t)$$

$$A(r;t) = A_0(r) + \delta A(r;t)$$

$$\phi(r;t) = \phi_0(r) + \delta \phi(r;t)$$

$$Q(r;t) = Q_0 + \delta Q(r;t):$$

f_0, A_0 , and ϕ_0 are the static solution found in the previous sections and δ denotes smallness compared to static solution. Here we are making a perturbation around the topological charge Q as well, which in the static case was taken to be 1. The new action is

$$S = \int d^4x \left[-\frac{1}{2} R + \frac{1}{2} (\partial_\mu \phi)^2 + e^4 \left(\frac{H^2}{3} - \frac{2C}{r^2} e^{2\phi} \cos Q \right) \right]$$

where H_{abc} has nonzero components

$$H_r = \frac{\phi_0 \sin Q}{2} \partial_r Q \quad \text{and} \quad H_t = \frac{\phi_0 \sin Q}{2} \partial_t Q$$

The linearized gravitational field equations obtained from the action do not lead to an unstable mode because a spherically symmetric gravitational field has no dynamical degrees of freedom. Explicit demonstration of this fact is given in [14].

After dropping the subscript 0 of the background solution, the linearized equation of motion for $\delta \phi$ is,

$$\frac{1}{f} \partial_\mu \partial^\mu \delta \phi + \frac{2C}{f^2} e^{2\phi} \delta \phi = 0$$

where $\partial = \partial/\partial x$ ($x = r/r_h$) and ϕ_0 has been scaled away. We have also scaled the time coordinate by a constant and taken the time dependence of $\delta \phi$ to be $e^{i\omega t}$. Then, after transforming to the tortoise coordinate $\frac{dy}{dx} = \frac{1}{fA}$, we obtain the equation for $\delta \phi(y)$ as

$$\frac{d^2}{dy^2} \delta \phi + (E - V) \delta \phi = 0$$

where $E = \omega^2$, and

$$V = \frac{1}{2x} \frac{d}{dx} (fA) + \frac{2fC}{x^4} e^{2\phi} x^2 r_h^2$$

This is one dimensional nonrelativistic schrodinger equation for a particle with mass = $\frac{1}{2}$ moving under the influence of the potential V . Instability of the solution corresponds to the existence of the bound states, $E < 0$, solutions of the static solution. But V is positive definite form most of the parameter space of the static solution. See figure 7. Thus in this region of parameter space, where C and/or r_h are small, a linear time dependent perturbation in the dilaton field leads to no instability.¹

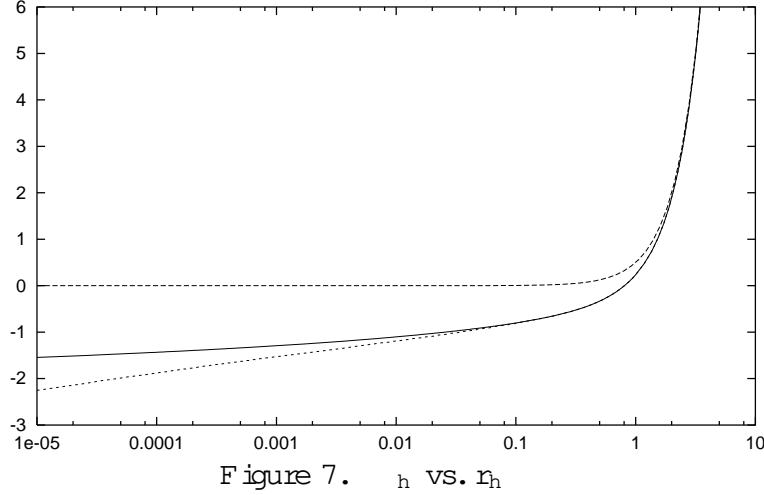


Figure 7. r_h vs. C . According to the remarks at the end of section 5 this figure can be looked upon as C vs. r_h with $\alpha_1 = 0$. Dashed line is the curve $r_h^2 = 2$, Hawking temperature bound on r_h with $C = 1$. Solid line is r_h^{\max} vs. r_h ; it determines the boundary of solution space i.e. no static solution exists for any point above the solid line. V is positive definite below the small-dashed line.

We next investigate the equation of motion for Q in the parameter space in which V is positive definite. Assuming the same time dependence as before the linearized equation of motion for Q can also be put into the form of the schrodinger equation as before with the potential energy function

$$V_Q(y) = A f B^2 - B^0(x) \frac{B}{2} \frac{d}{dx} (fA) - 3fx^2 r_h^4 C e^6 x^2 r_h^2$$

where $B(x) = 2^{-\alpha_1(x)} + 1 = x$. Here we have set $\alpha_1 = 2$ for convenience. To study V_Q it is convenient to think² of the representation in which $(r_h; C)$ is varied and $\alpha_1 = 0$. One should imagine figure 7 as C vs. r_h with $r_h \neq 1$ being $C \neq 0$. Now the last term in V_Q will be small when C and/or r_h are small whereas other terms do not depend explicitly on C or r_h . Thus the effect of the last term in V_Q will show up for the points in upper right of figure 7. Figure 8 shows a typical V_Q when C and/or r_h is small; it has a well |

¹ We believe that even in the region of parameter space which makes V negative no bound state with $E < 0$ is possible. The reason is that when V does become negative it is in the form of a shallow well surrounded by a high barrier and a small barrier.

² Because $C e^6$ appears in V_Q there is no simple transformation between the parameter space where C is fixed and α_1 varied and that where α_1 is fixed and C varied. However, when one considers which part of the static solution space is stable under perturbation, it is consistent to use the simple transformation rule given at the end of section 5.

which we will refer to as the "primary" well | followed by a barrier. From now on we will consider varying $(r_h; C; \hbar) = (0.077161; 1; 1)$.

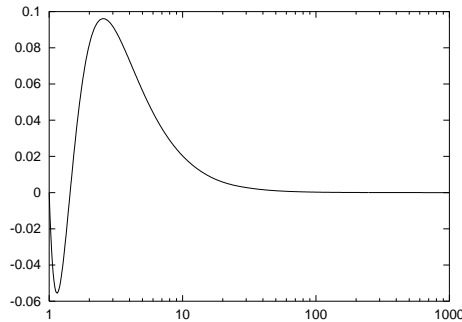


Figure 8. V_Q vs. x $(r_h; C; \hbar) = (0.077161; 1; 1)$

The effect of r_h and \hbar when they are larger (i.e. when they are in the upper right of figure 7) is to introduce a "secondary" well whose location depends on r_h . In general this secondary well gets deeper as r_h and \hbar gets bigger and moves to the left as r_h gets bigger. See figures 11a,b,c,d. If there is any bound state of V_Q the particle will be localized in the primary well or the secondary well. Since big r_h and \hbar give a deep secondary well, we start looking for bound states for such cases.

To find the bound states of V_Q it is numerically simpler to use the original x coordinate. As $x \rightarrow 1$ the solution for Q is e^{-x} and the linearized equation of $q = Q e^{-x}$ is

$$q'' - (a + 2x)q' + (x^2 + a - b)q = 0$$

where $x = d/dx$,

$$a = 2B(x) - \frac{1}{2} \ln^2(fA) \quad \text{and} \quad b = \frac{x^2}{fA} - \frac{3x^2 r_h^4}{A} C e^{6x} x^2 r_h^2$$

The wave function in the schrodinger equation is related to q via $\psi = (q/x)e^{-x}$.

For arbitrary value of x and arbitrary potential V_Q , no regular solution of ψ will be possible. We call ψ a regular solution if it goes to zero sufficiently fast as $x \rightarrow 1$ and $x \rightarrow \infty$. We find that for a deep enough secondary well of V_Q and a discrete set of positive values of x regular solutions exist. These regular solutions are the bound states we are looking for.

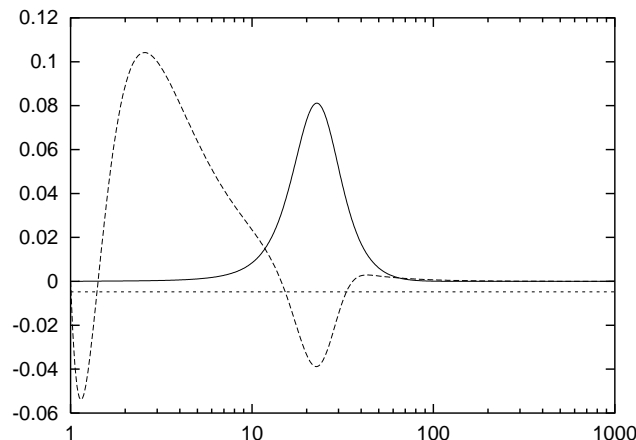


Figure 9. V_Q and ψ vs. x $(r_h; C; \hbar) = (0.077161; 1; 0.875)$

Solid line is the wave function of the ground state and horizontal line the energy level.

As shown in figure 9 the wave function is localized around the secondary well, and this is evidence that no bound state will be possible when the secondary well is shallow enough. Therefore for a fixed r_h there may be bound states when μ_h is close to μ_h^{max} but as $\mu_h^{max} \rightarrow 1$ bound states will disappear. For a fixed r_h we can graph μ of the ground state against μ_h and by extrapolating find the zero of that graph, μ_h^0 . See figure 10. For $\mu_h < \mu_h^0$ no bound state is possible and hence the solution is stable.

7. Summary

We have presented the evidence for the existence of scalar hair of a black hole in the presence of string instantons which couple to a topological gauge potential. The spacetime action that we use includes an effective interaction due to the string instantons wrapping around the Euclidean black hole. Measurement of the dilaton charge of the black hole can be looked upon as an indirect detection of the topological axion charge of the black hole. For example, if a "dilaton ball" held at a large distance from the black hole experiences an attractive force towards the black hole in excess of the gravitational force the dilaton charge of the black hole will be ascertained, and hence the axionic charge.

Acknowledgements

JT would like to thank D. K. Astor and S. Giddings for useful conversations. This work is supported in part by NSF Grant NSF-THE-8714-684-A01.

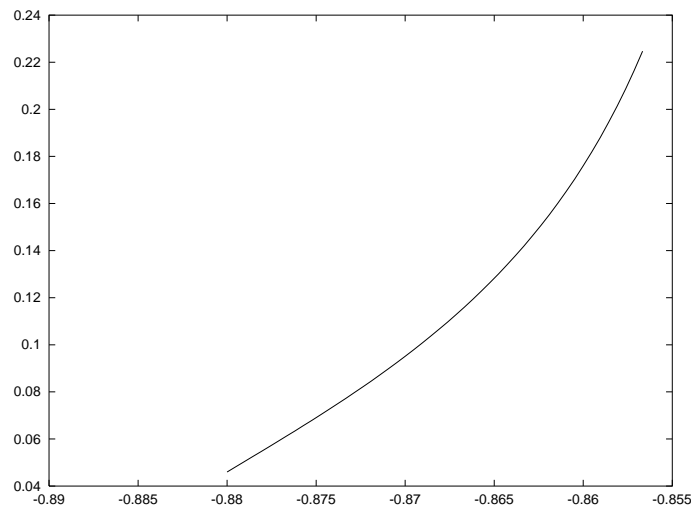


Figure 10. μ vs. μ_h ($r_h; C$) = (0.077161; 1) μ_h^0 = 0.892

Because there is one-to-one correspondence between C and μ_h (of the static solution) this figure can be roughly looked upon as μ vs. C with $\mu_1 = 0$.

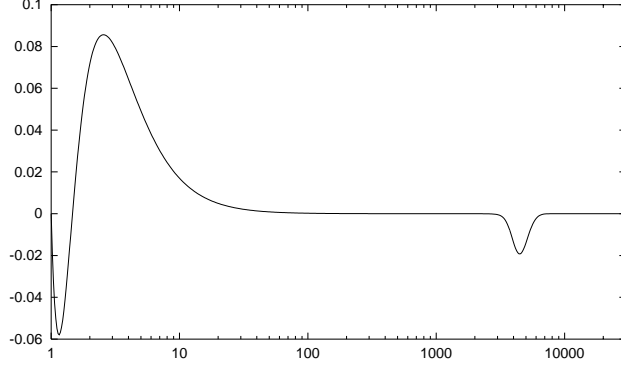


Figure 11a. V_Q vs. x $(r_h; C; h) = (0.0005265; 1; 1.33594)$

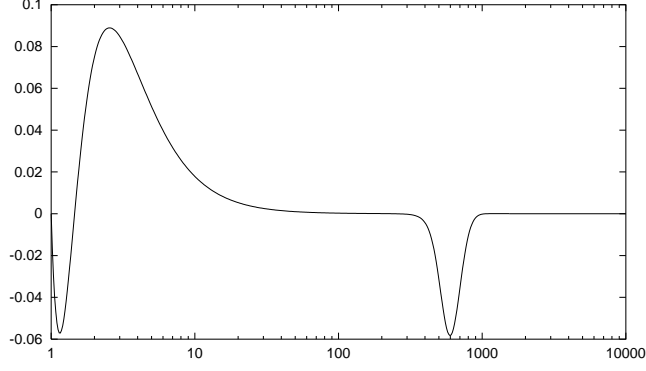


Figure 11b. V_Q vs. x $(r_h; C; h) = (0.003679; 1; 1.194)$

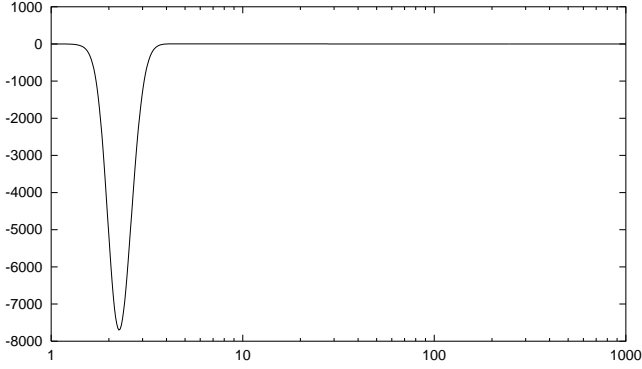


Figure 11c. V_Q vs. x $(r_h; C; h) = (1; 1; 0.23)$
 r_h 's of figures a,b,c lie on the small dashed line of figure 7.

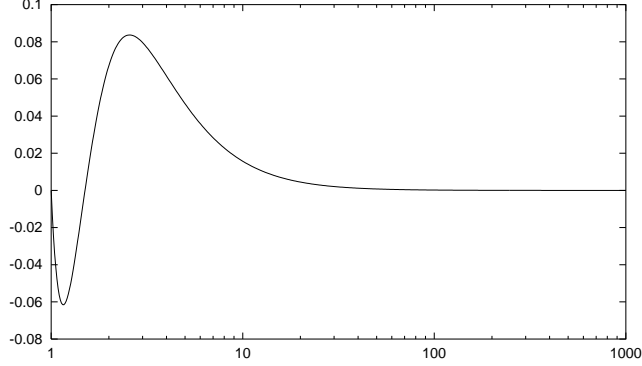


Figure 11d. V_Q vs. x $(r_h; C; h) = (1; 1; 1.194)$

References

- [1] Wald, R. M. 1984, *General Relativity* (Chicago: University of Chicago Press), and references therein.
- [2] Bekenstein, J. D. 1972, "Transcendence of the Law of Baryon-Number Conservation in Black-Hole Physics," *Phys. Rev. Lett.* 28, 452-455.
- [3] Adler, S. L., and Pearson, R. B. 1978, "No-hair theorems for the Abelian Higgs and Goldstone models," *Phys. Rev. D* 18, 2798-2803.
- [4] Bizon, P. 1990, "Colored Black Holes," *Phys. Rev. Lett.* 64, 2844-2847.
- [5] Smoller, J. A., Wasserman, A. G., and Yau, S. T. 1993, "Existence of black hole solutions for the Einstein-Yang-Mills Equations," *Comm. Math. Phys.* 154, 377-401.
- [6] Lee, K., Nair, V. P., and Weinberg, E. 1992, "Black Holes in Magnetic Monopoles," *Phys. Rev. D* 45, 2751-2761. (hep-th 9112008)
- [7] Kastor, D., and Traschen, J. 1992, "Horizons Inside Classical Lumps," *Phys. Rev. D* 46, 5399-5403. (hep-th 9207070)
- [8] Garfinkle, D., Horowitz, G. T., and Strominger, A. 1991, "Charged Black Holes in String Theory," *Phys. Rev. D* 43, 3140-3143. erratum 45, 3888, 1992.
- [9] Shapere, A., Trivedi, S. and Wilczek, F. 1991, "Dual Dilaton Dyons," *Mod. Phys. Lett. A* 6, 2677-2686.
- [10] Giddings, S. B., Harvey, J. A., Polchinski, J. G., Shenker, S. H., and Strominger, A. 1994, "Hairy Black Holes in String Theory," *Phys. Rev. D* 50, 6422-6426 (hep-th 9309152).
- [11] Bowick, M. J., Giddings, S. B., Harvey, J. A., Horowitz, G. T., and Strominger, A. 1988, "Axionic Black Holes and an Aharonov-Bohm Effect for Strings," *Phys. Rev. Lett.* 61, 2823-2826.
- [12] Press, W. H., Teukolsky, S. A., Vetterling, W. T. and Flannery, B. P. 1992, *Numerical Recipes: The Art of Scientific Computing* (Cambridge: Cambridge University Press).
- [13] Heusler, M. 1996, "No-Hair Theorems and Black Holes with Hair" (gr-qc 9610019)
- [14] Straumann, N. and Zhou, Z. H. 1990, "Instability of the Bartnik-McKinnon Solution of the Einstein-Yang-Mills Equations," *Phys. Lett. B* 237, 353-356.